

## Microstructural origin of the dielectric breakdown strength in alumina: A study by positron lifetime spectroscopy

A. Si Ahmed<sup>a,\*</sup>, J. Kansy<sup>a,b</sup>, K. Zarbout<sup>a</sup>, G. Moya<sup>a</sup>, J. Liebault<sup>c</sup>, D. Gœuriot<sup>c</sup>

<sup>a</sup> L2MP, U.M.R./CNRS 6137, Université Paul Cézanne (Aix-Marseille III),

Faculté des Sciences et Techniques, Case 222, Avenue Escadrille Normandie Niémen, F 13397 Marseille, France

<sup>b</sup> Institute of Physics of Metals, Silesian University, Bankowa 12, Pl 40-007 Katowice, Poland

<sup>c</sup> Ecole Nationale Supérieure des Mines de Saint Etienne, F 42023 Saint Etienne, France

Available online 25 March 2005

### Abstract

The dielectric breakdown strengths of two series of sintered alumina samples of low and high impurity content (with Si being the dominant element) and single crystal of low impurity level are compared with positron lifetime measurements. It is found that, in sintered alumina, the breakdown strength increases linearly with increasing concentration of positron traps at grain boundaries. These traps are likely clusters containing negatively charged cationic vacancies, which are induced by silicon dissolution into  $\text{Al}_2\text{O}_3$ . Therefore, the improvement of the breakdown strength can be traced to silicon segregation at grain boundaries. More precisely, it is deduced that the dissolution of Si impurity into  $\text{Al}_2\text{O}_3$ , when it is compensated by a cationic vacancy  $V_{\text{Al}}'''$ , is responsible for such an improvement. A solubility of Si in  $\text{Al}_2\text{O}_3$ , achieved during the firing schedule of the sintering process, and which does not take into account enhanced solubility caused by mutual compensation of Si with lower valence foreign cations such as Ca and MgO, is estimated at 120 ppm.

© 2005 Elsevier Ltd. All rights reserved.

**Keywords:** Sintering; Grain boundaries; Dielectric properties; Positron annihilation;  $\text{Al}_2\text{O}_3$

### 1. Introduction

Positron annihilation lifetime spectroscopy (PALS) is sensitive to vacancy-like defects in materials.<sup>1</sup> In oxides, the dissolution of foreign cations, greater or lesser in valence than the host cation, requires that charged point defects be created in order to preserve electrical neutrality. Neutral and negatively charged vacancies (or vacancy clusters) act as positron traps. In  $\text{Al}_2\text{O}_3$ , only the cations greater in valence than Al, such as Si, can spawn negatively charged vacancies,<sup>2,3</sup> namely the cationic vacancies  $V_{\text{Al}}'''$ . In addition, it has been shown that the defect structure achieved during the firing schedule of the sintering process comprises, among other defects that are not felt by positrons, isolated  $V_{\text{Al}}'''$  as well as neutral and negatively charged defect complexes containing cationic vacancies.<sup>3,4</sup> As a result, PALS measurements can be traced to the Si concentration or, more precisely, to the frac-

tion of that concentration whose dissolution is compensated by  $V_{\text{Al}}'''$ .

In previous works,<sup>4,5</sup> PALS measurements were carried out at room temperature in two series of sintered  $\text{Al}_2\text{O}_3$  samples. In both materials, Si was the dominant impurity (i.e., 90 ppm and 1500 ppm). Two lifetime components of 137 ps and 400 ps were resolved for both series, which can be interpreted as an indication that the nature of positron traps are identical in the two materials. The shorter lifetime was assigned to  $V_{\text{Al}}'''$  located within the grain and the other to grain boundaries clusters (i.e., likely  $V_{\text{Al}}'''$  associated with segregated impurities<sup>4</sup>). The dielectric breakdown strengths (measured at room temperature) of the same sintered samples and of single crystal have also been reported.<sup>6,7</sup>

The purpose of this work is to improve the understanding of the microstructural origin of the dielectric breakdown strength by calling for the nature and localisation of defects that are provided by PALS measurements. An earlier attempt to establish a relation between the breakdown strength and PALS measurements has been reported.<sup>7</sup> In this first

\* Corresponding author. Tel.: +33 4 91 28 86 14; fax: +33 4 91 28 27 98.  
E-mail address: [a.siahmed@univ.u-3mrs.fr](mailto:a.siahmed@univ.u-3mrs.fr) (A. Si Ahmed).

approach, the *two state trapping model*, which considers only one trapping process, was used. In the present work, the results derived from a more complete description<sup>4,5</sup> (i.e., the *three state trapping model*<sup>8</sup>) are utilised. This description allows an access to two trapping processes, which are expected to stem from positron trapping in defects located within the grain and at grain boundaries. Hence, the particular role of the grain boundaries and of the segregated elements can be investigated.

## 2. Materials preparation and experiments

### 2.1. Materials characteristics and preparation

The sintered materials referred below as “doped” samples contained SiO<sub>2</sub> (1497 ppm), MgO (723 ppm), CaO (686 ppm), Fe<sub>2</sub>O<sub>3</sub> (415 ppm) and Na<sub>2</sub>O (404 ppm). The other ones considered as “pure” contained SiO<sub>2</sub> (90 ppm) Na<sub>2</sub>O (40 ppm) and background impurities (of total amount near 20 ppm). Sintering was performed in air and the different grain diameters were reached by controlling the firing schedule.<sup>6</sup> In addition, we used Al<sub>2</sub>O<sub>3</sub> single crystal which has about the same impurity level as the “pure” sintered materials.

### 2.2. Breakdown strength determination

The specimen were tested after sintering. Each sample was clamped between two hemispherically ended brass electrodes. The measurements were carried out at room temperature in transformer oil under an alternative current (50 Hz). The details of the experimental set up and measurement procedure were described in Ref. <sup>6</sup>.

The breakdown strength  $E_c$  as a function of specific surface of grain boundaries ( $s_{GB}$ ) is plotted in Fig. 1. The specific surface is estimated by assuming grains of spherical shapes, i.e.,  $s_{GB} = 3/R$  where  $R$  is the mean radius of grains. For the “pure” samples,  $E_c$  seems to be constant at value about 15.2 kV/mm whereas for the “doped” ones a linear dependence,  $E_c = 0.454s_{GB} + 12.16$  kV/mm, is observed. The value of the breakdown strength of a single crystal (12.3 kV/mm)

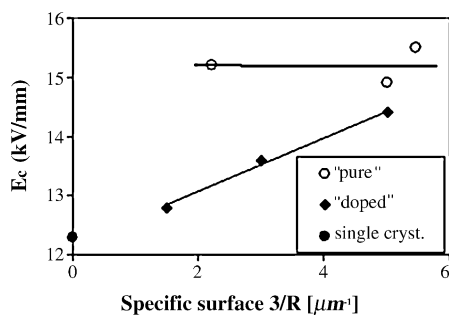


Fig. 1. Breakdown strength versus specific surface of grains in alumina samples of different impurity contents.

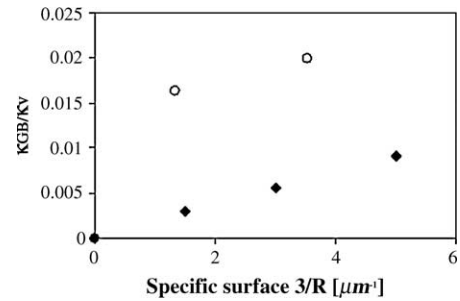


Fig. 2. The ratio of positron trapping rates  $\kappa_{GB}/\kappa_V$  into defects at grain boundaries and into vacancies inside grains versus specific surface of grains (symbols as in Fig. 1).

is also given, which evidently corresponds to an infinite grain radius.

### 2.3. Positron lifetime measurements: analysis and results

For the PALS experiments, the same single crystal and “doped” samples were taken as in the breakdown strength measurements. However, in the case of “pure” materials, two other samples were used. These samples have the same impurity contents as those of Fig. 1, but differ by their grain size.<sup>4</sup> The positron lifetime spectra were recorded at room temperature using a conventional fast–fast coincidence system. The spectra were measured in 2000 channels (calibration 27 ps/channel and FWHM of 270 ps) and collected about  $6 \times 10^6$  counts. They were analysed via a *LT v.9 program*,<sup>9</sup> in which the *three-state trapping model*<sup>8</sup> was introduced into the source code. The three states refer to different locations of positron annihilation (i.e., in the bulk material, in vacancies within the grains and in defects at grain boundaries). In the case of “doped” samples, the first state (annihilations in the bulk) turned out to be negligible. In single crystal, the third process (annihilation at grain boundaries) is considered equal to zero as there are no grain boundaries. The details of the experiments and their analyses have been described in our previous works.<sup>4,5</sup>

In Fig. 2, the ratio  $\kappa_{GB}/\kappa_V$  (where  $\kappa_{GB}$  and  $\kappa_V$  are respectively the positron trapping rates in defects at grain boundaries and in defects within the grain) is plotted as a function of  $s_{GB}$ . Only these PALS spectrum parameters are of interest for the scope of the following discussion.

## 3. Discussion

From the comparison of Figs. 1 and 2, one can observe a quite similar dependence of  $E_c$  and  $\kappa_{GB}/\kappa_V$  on the specific surface  $s_{GB}$ . This suggests a correlation between  $E_c$  and the ratio  $\kappa_{GB}/\kappa_V$ . According to the trapping model, this ratio is proportional to  $c_{GB}/c_V$ , where  $c_{GB}$  and  $c_V$  express, respectively, the concentrations of positron traps at grain boundaries and within the grains. The proportionality factor is expected to be of order of unity. For a given type of samples (“doped”

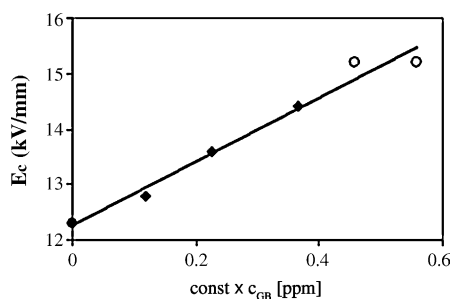


Fig. 3. Breakdown strength as a function of defect concentration at grain boundaries. The straight line represents the best fit to the points (see text) (symbols as in Fig. 1).

or “pure”), the relative variation of  $c_V$  is not significant (i.e., almost independent of the grain size and hence of the firing schedule<sup>4</sup>). In contrast,  $c_{GB}$  is expected to be much more sensitive to the extent of segregation. Indeed, the segregated elements are confined within a rather small volume (compared to the volume of the entire grain whose diameter lies between 1 and 4.5  $\mu\text{m}$ ) characterised by a grain boundary width of about  $10^{-9}$  m. Consequently, the variations of the ratio  $\kappa_{GB}/\kappa_V$  reflect mainly the changes of the concentration of positron traps,  $c_{GB}$ , at grain boundaries.

To determine the changes of  $c_{GB} = \text{const} \times c_V \kappa_{GB}/\kappa_V$ , the concentration  $c_V$  within the grains in “pure” and “doped” samples must be known. For “pure” samples,  $c_V$  can be estimated with some assurance from the Si content,<sup>4</sup> which is well below its solubility limit,<sup>10,11</sup> at about 28 ppm. However, in the case of “doped” samples,  $c_V$  cannot be evaluated on the basis of impurity content, because it is so high that  $c_V$  achieves its ultimate value, which is determined by the solubility of Si. Assuming that the correlation between  $E_c$  and  $c_{GB}$  is the same for “pure” and “doped” samples, one could estimate the unknown value  $c_V$  for “doped” samples by fitting a straight line to all of the experimental points in the plot  $E_c$  against  $c_{GB} = \text{const} \times c_V \kappa_{GB}/\kappa_V$  (Fig. 3). The best fit can be obtained if  $c_V$  in “doped” samples is 40 ppm. Taking into account that a vacancy is induced by the dissolution of three Si atoms,<sup>4</sup> one can estimate the lower limit of the solubility of Si at 120 ppm. Here, it must be reminded that Si is the only foreign element whose dissolution can give birth to negatively charged cationic vacancies  $V_{Al}'''$  and hence to positron traps.<sup>2,3</sup> This value is lower than the solubility reported in Refs. <sup>10,11</sup> under sintering conditions close to ours. There, Si level in the range 200–300 ppm was found just sufficient for the formation of glassy grain boundary films. We have to acknowledge that PALS cannot reflect the actual solubility limit of Si in the “doped” samples. Indeed, some fraction of silicon could be prevented from inducing  $V_{Al}'''$ , due to possible mutual compensation of Si with lower valence impurities,<sup>2</sup> such as Ca and Mg, which are present in substantial amount in the “doped” samples. Such mutual compensations were also called for an explanation of the solubility enhancement of Si in sintered alumina.<sup>11,12</sup> Therefore, the departure of the value derived from PALS (120 ppm) from the actual solu-

bility (200–300 ppm) could be seen as an assessment of the mutual compensation effects.

The correlation which emerges from Fig. 3 indicates that the breakdown strength is improved by the existence of grain boundaries. However, it illustrates that such an improvement can be furthermore traced to the concentration of positron traps at grain boundaries. Since the positron traps are induced by Si dissolution into  $\text{Al}_2\text{O}_3$ , the breakdown strength is also sensitive to silicon segregation. Such a correlation appears as a signature of the effect of the microstructural development during the sintering process on a macroscopic property, i.e. the dielectric breakdown strength. However, a relevant question arises (i.e., why the concentration of positron traps seems higher in the “pure” samples, with only 90 ppm of Si, than in the “doped” ones, with 1500 ppm of Si, as it is indicated in Fig. 3). Here again, mutual compensation of Si with Ca and Mg could be responsible for such effect. Furthermore, preferential segregations, and in particular of Ca, which exhibits the strongest tendency for segregation<sup>13</sup> that is characterised by an enrichment ratio higher than 1300, could interfere via the reduction of Si concentration at grain boundaries. We have to acknowledge that, at this stage, the present work does not lead to a unique explanation. Nevertheless, from the above correlation, one can speculate that the dissolution of Si impurity into  $\text{Al}_2\text{O}_3$ , when it is compensated by a cationic vacancy  $V_{Al}'''$ , plays a significant role in the improvement of the breakdown strength of sintered alumina. Further unambiguous clarification of this role requires investigations using series of materials of well defined impurity contents. To this end, it is felt that this work provides a suitable framework, which can also be geared to the optimisation of the dielectric properties of sintered alumina.

## References

- Hautojärvi, P., ed., *Positron in Solids*. Springer-Verlag, Berlin, 1979.
- Grimes, R. W., Solution of MgO, CaO and  $\text{TiO}_2$  in  $\alpha\text{-Al}_2\text{O}_3$ . *J. Am. Ceram. Soc.*, 1994, **77**, 378–384.
- Lagerlöf, K. P. D. and Grimes, R. W., The defect chemistry of sapphire ( $\alpha\text{-Al}_2\text{O}_3$ ). *Acta Mater.*, 1998, **46**, 5689–5700.
- Moya, G., Kansy, J., Si Ahmed, A., Liebault, J., Moya, F. and Gœuriot, D., Positron lifetime measurements in sintered alumina. *Phys. Stat. Sol. (a)*, 2003, **198**, 215–223.
- Si Ahmed, A., Kansy, J., ZARBOUT, K., Moya, G. and Gœuriot, D., Positron trapping within the grain boundaries in sintered alumina of high impurity content. *Mater. Sci. Forum*, 2004, **445–446**, 177–179.
- Liebault, J., Vallayer, J., Gœuriot, D., Treheux, D. and Thevenot, F., How the trapping of charges can explain dielectric breakdown performances of alumina ceramics. *J. Eur. Ceram. Soc.*, 2001, **21**, 389–397.
- Liebault, J., Si Ahmed, A., Kansy, J., Gœuriot, D. and Moya, G., Correlation between the dielectric breakdown strength and the positron lifetime measurements in sintered alumina. In *Proceedings of the 4th International Conference on Electric Charges in Non-conductive Materials*. Société Française du Vide, Paris, 2001, pp. 165–168.
- Krause-Rehberg, R. and Leipner, H. S., *Positron Annihilation in Semiconductors*. Springer-Verlag, Berlin, 1999, pp. 89–91.

9. Kansy, J., Microcomputer program for analysis of positron annihilation lifetime spectra. *Nucl. Instrum. Methods A*, 1996, **347**, 235–244.
10. Bae, S. I. and Baik, S. J., Determination of critical of silica and/or calcia for abnormal grain growth in alumina. *J. Am. Ceram. Soc.*, 1993, **76**, 1065–1067.
11. Gavrilov, K. L., Bennison, S. J., Mikeska, K. R., Chabala, J. M. and Levy-Setti, R., Silica and magnesia dopant distributions in alumina by high-resolution scanning secondary ion mass-spectrometry. *J. Am. Ceram. Soc.*, 1999, **82**, 1001–1008.
12. Gavrilov, K. L., Bennison, S. J., Mikeska, K. R. and Levy-Setti, R., Grain boundary chemistry of alumina by high-resolution imaging SIMS. *Acta Mater.*, 1999, **47**, 4031–4039.
13. Dörre, E. and Hübner, H., *Alumina*. Springer-Verlag, Berlin, 1979, pp. 69–73.